

# Design of polymer BenzoCycloButene (BCB) based silicon photonic MZI waveguide for label-free biosensing

S. PRASANNA KUMAAR<sup>1,\*</sup>, A. SIVASUBRAMANIAN<sup>2,\*</sup>

<sup>1</sup>*Department of Electronics and Communication Engineering, Kumaraguru College of Technology, Coimbatore- 641049, India*

<sup>2</sup>*School of Electronics Engineering, Vellore Institute of Technology, Chennai 600127, India*

The proposed cost-effective polymer-based Mach-Zehnder Interferometer (MZI) refractive index (RI) sensor with rib-slot waveguide offers high sensitivity with a simple fabrication process. Due to recent demand in point-of-care biosensor at low cost, we need to identify silicon wafer-based polymer material. Hence, we designed a waveguide with Benzo Cyclobutene core and polymethyl methacrylate (PMMA) clad on a silicon wafer. The proposed gradient rib-slot waveguide structure of 2.18  $\mu\text{m}$  wide and 1  $\mu\text{m}$  thick, holds liquid sample in the sensing region effectively. In MZI architecture, reference arm of 1 cm and sensing arm at length of 1.3 cm with analyte refractive index of cancer cell (1.401) and Influenza A virus (1.48) are applied with thickness range from 400 nm to 90 nm. Through Finite-difference time domain (FDTD) analysis, effective mode index of BCB core are investigated and sensitivity results are calculated. Detection of cancer cell and Influenza A are plotted in transmission spectrum with normal human serum RI (1.35). This novel polymer waveguide structure achieves the MZI sensitivity of  $2.5 \times 10^5$  nm/RIU, which is higher in this segment of refractive index biosensing.

(Received July 28, 2023; accepted April 8, 2024)

*Keywords:* Mach-Zehnder Interferometer, Refractive index sensor, Benzo Cyclobutene, Waveguide sensor

## 1. Introduction

In recent times genetic and viral diseases are an imminent threat. Detection of cancer cell and viruses such as Influenza A type have challenged the medical field to develop a low-cost label free biosensor [1]. In India, a recent report of the National Cancer Registry Programme, 2020 by Indian council of medical research (ICMR) and National centre for disease information and research (NCIDIR), out of nine Indians one will be developed cancer in lifetime [2]. Diagnosis of cancer at early stage and proper follow up will decrease the severity of the disease. Early detection of cancer and Influenza in present post-pandemic is possible with modern techniques. Many such reports are reported in the literature on detection of different biomolecules, virus, and bacteria etc. [3][4].

In photonics, waveguide-based biosensor now more than ever, new materials and design prospects are increasing in disease diagnosis applications [5]. In this context, developing high sensitive and inexpensive biosensor integrated in mobile phone has been the subject of current research efforts [6] [7]. Biosensors are classified based on different transduction methods [8]. In optical biosensors chemical-related reagents are not added in to the sample [9]. This active sample will increase the sensitivity of sensor to quantify biomolecule present in sample [10]. In integrated photonic sensors two main techniques are used, namely absorption sensing and refractive index sensing (RI) [11][12]. In refractive index sensing only the real part  $n$  will be detected from the

analyte. And also RI based photonic sensor use small volume of the sample  $n$  placed in waveguide surface [5]. Real part  $n$  in analyte refractive index is linked to concentration not exactly related to total sample mass [13] [14]. Therefore, refractive index (RI) based integrated photonic sensor has good possibility for biological detection [15]. Another benefit of RI sensors is that minor changes in real part  $n$  over short distances can result in significant changes in phase of propagating wave. Due to the density and viscosity of the biomolecule, the spread of this sample over the waveguide surface will be not be uniform. The analyte concentration we proposed is from the Refractive index which can be detected by various optical devices at very high sensitivities [16]. In photonic waveguide based refractive index sensors most commonly used devices are Mach-Zehnder Interferometer (MZI) and micro ring resonators (MRR) [5]. But photonic RI sensors are not specific i.e they only calculate the refractive index  $n$  value and are unable to identify the substance or diseases that caused change in effective index. Thus, in Photonic waveguide sensor sample holder absorbs the liquid sample (analyte) reduces the sensitivity. To solve this problem, especially in biosensing, polymer based integrated sample holder is used at the edges of the waveguide surface [17]. The integration of polymer materials in SOI platforms is one of the novel areas of research that have been investigated in the literature review to address this limitation. Several polymer low refractive index, high biocompatibility, and ease of processing have made them an effective replacement for traditional silicon-based

techniques. By enhancing the detection limit by increasing the overlap of the evanescent field with the analyte, the integration of polymers with SOI waveguides can considerably increase the sensitivity of the sensors. The development of low-cost, high-sensitive photonic RI sensor is widely preferred because the restoration of the biosensor after use, cleaning with a solution is very difficult and time-consuming process [18]. MZI-based photonic sensors, does not require complex process to fabricate and it is a cost-effective device structure too [5]. Integration of MZI configuration with other optical and opto-electrical components is simple, and detection of variation in the transmission spectrum of the different disease samples (analyte) are accurate [19]. Since the MZI-based sensors use evanescent field probing scheme, to detect the disease with strong evanescent wave absorption into the analyte, it achieves high waveguide sensitivity [20]. Some slot waveguide, subwavelength grating waveguides and novel waveguides have been proposed and reported in recent works of literature [21] [22].

A PMMA cladding layer is typically used to separate the reference arm of a MZI sensor from the analyte in order to increase sensitivity, creating an asymmetric MZI configuration [4]. The sensitivity of the sensor as an interferometric device is significantly impacted by the optical path difference (OPD) between the two arms. In particular, the OPD of the MZI were carefully designed to cause a dip in transmission spectrum at an important working point in order to pursue an ultra-high sensitivity [23]. Due to fabrication mismatch of the sensor, dip in transmission spectrum need a precise characterization. To achieve accurate sensing, expensive facilities are needed, which results in a high cost of the sensor. The aim of the work is to create a liquid refractive index sensor with availability of wide range of affordable polymer materials. In order to achieve a high sensitivity, a clear and simple asymmetric MZI constructed with a standard rib-slot waveguide [24]. Here, the BCB core PMMA cladding reference arm and BCB core sensing arm length are consequently optimized with configurable refractive index of waveguides can be made for label free biosensing [25][26].

The objective of the proposed polymer MZI biosensor design is to create a cost-effective photonic biosensor. In future, this design of biosensor will motivate the researchers to integrate them with mobile phones [6] [7]. The proposed waveguide structure analysed with physical environment factors like analyte transportation and temperature. In rib-slot waveguide waveguide 2.18  $\mu\text{m}$  wide and 1  $\mu\text{m}$  thick benzo cyclobutene (BCB) core and polymethyl methacrylate (PMMA) cladding layer. By etching PMMA for sensing window to hold the liquid sample effectively without any leakages at edges. This results in increase in the interaction of light with the sample, which detects the changes in sample and increase

the number of peaks in transmission spectrum. The sensor exhibits high sensitivity of  $2.5 \times 10^5$  using MZI architecture. The transmission spectrum detected the cancer cell and Influenza A virus over normal human blood.

## 2. Materials and methods

The proposed polymer benzo cyclobutene (BCB) core waveguide grown in buffer silicon oxide (SiO<sub>2</sub>) wafer with polymethyl methacrylate (PMMA) as cladding layer. The physical properties of polymer is effectively simulated in Lumerical FDTD with refractive index of BCB 1.5370, and PMMA 1.4710. Even though Silicon and silicon nitride waveguide offers higher refractive index contrast, the proposed polymer rib slot waveguide provides better sensitivity [27]. The novelty of this waveguide design is in Z direction, where the thickness of waveguide increases and analyte thickness is reduced from 400 nm to 90 nm is shown in Fig. 1. This optimized gradient rib-slot waveguide are analysed for physical environment factors of the sensor for possible integration on point-of care device [28]. The viscosity and density of the sample is very small and not constant in the real environment. By considering all these aspects we proposed the polymer waveguide with integrated analyte holder, etching PMMA cladding layer in sensing arm which holds the sample effectively shown in Fig. 2 (a) and Fig. 2 (b).

Large core waveguides confines light in the core with small loss, reduces the sensitivity of the sensor [29]. Therefore, the widths of the MZI reference arm and sensing arm of BCB waveguide are carefully designed and the optimized widths are analyzed and chosen in order to manage the waveguide sensitivity and the propagation loss while simultaneously accommodating only the fundamental mode.  $W_{\text{sensing}} = 2.18 \mu\text{m}$  and  $W_{\text{ref}} = 2.5 \mu\text{m}$  respectively, the height of BCB core  $h = 1 \mu\text{m}$  and  $L_{\text{ref}} = 1 \text{ cm}$ ,  $L_{\text{sensing}} = 1.3 \text{ cm}$ .

### 2.1. Evaluation of sensor sensitivity

Lumerical FDTD accurately simulates physical structure and electromagnetic wave propagation in the core. Computational electromagnetics has emerged as a key field of research in the design of effective sensing platforms [30], [31]. In gradient rib – slot waveguide, mode profile overlaps above the waveguide structure with analytes Fig. 2 (b) shows side view. By this evanescent wave penetrates in bulk sample and the change in effective index ( $n_{\text{eff}}$ ) and refractive index of sample ( $n_c$ ) are measured as bulk sensitivity [32], [33].

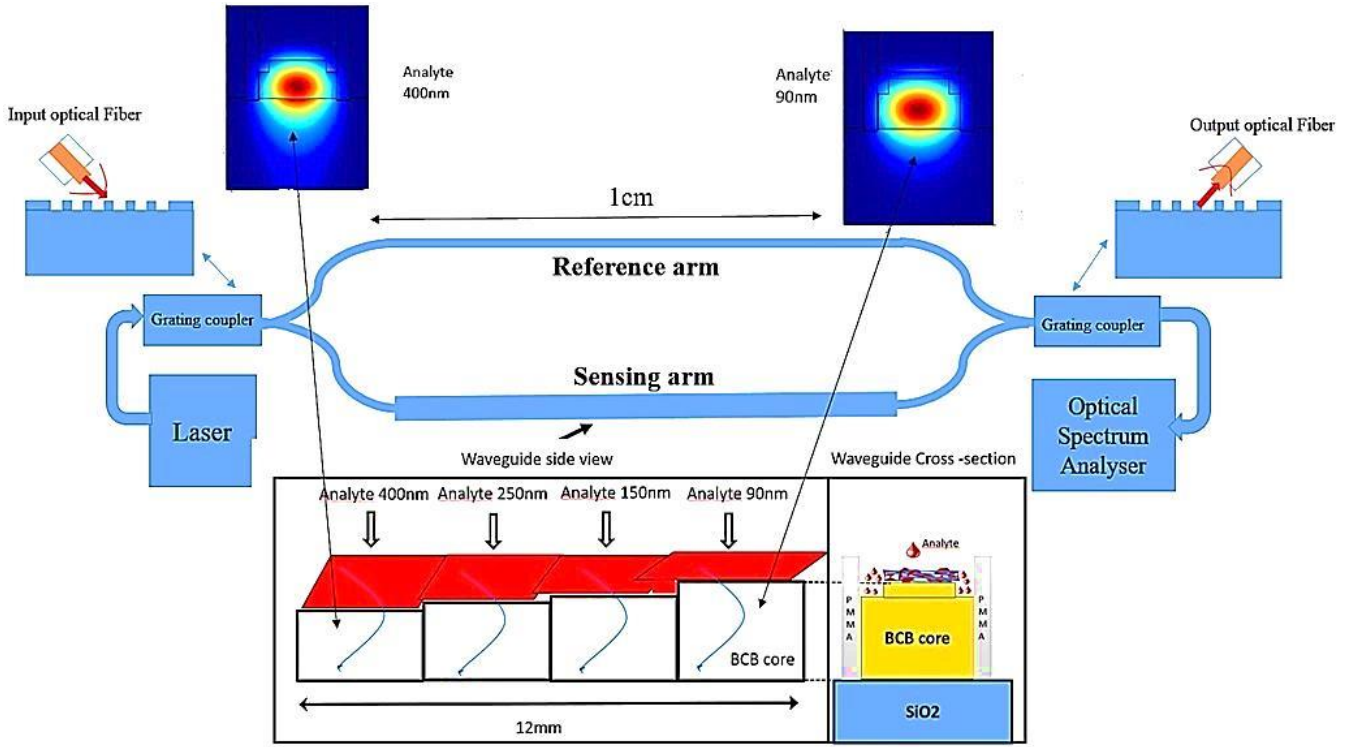


Fig. 1. Mach-Zehnder Interferometer (MZI) sensor architecture with rib-slot (color online)

$$\varphi = \frac{2\pi}{\lambda} (n_{eff}[ref]L_{ref} - n_{eff}[sensing]L_{sensing}), \quad (1)$$

In MZI polymer waveguide biosensor operating at  $\lambda = 1550$  nm, the quasi TE mode effective index are calculated for different analyte thickness and refractive index (RI) ranging from 1.35 to 1.48 [34]. This proposed polymer waveguide has dips in transmission periodically that correspond to destructive interference when the phase changes ( $\varphi$ ). Based on equation (1) wavelength dip in reference arm and sensing arm are obtained in equation (2)[35].

$$\lambda_{trans\ dip} = \frac{2}{m} (n_{eff}(ref)L_{ref} - n_{eff}(sensing)L_{sensing}), \quad (2)$$

The change in the analyte refractive index  $n_l$  which leads to change in  $n_{eff}(sensing)$  in sensing arm, which results in dip shift in transmission spectrum  $\Delta \lambda_{trans\ dip}$ . Based on the wavelength, and effective index, the equation (4)  $\lambda_{trans\ dip} + \Delta \lambda_{trans\ dip}$  can be written as equation (3).

$$\frac{\Delta n_l}{\Delta \lambda_{trans\ dip}} \frac{\partial n_{eff}(sensing)}{\partial n_l} \lambda_{trans\ dip} L_{sensing} = [n_{g\ ref} L_{ref} - n_{g\ sensing} L_{sensing}], \quad (3)$$

Based on equation (2) and equation (3)  $\Delta \lambda_{trans\ dip}$  can be written as

$$\begin{aligned} & \lambda_{trans\ dip} + \Delta \lambda_{trans\ dip} \\ &= \frac{2}{m} \left[ \left( n_{eff}(ref) \Delta \lambda_{trans\ dip} \frac{\partial n_{eff}(ref)}{\partial \lambda} \right) L_{ref} \right. \\ & \quad - \left( n_{eff}(sensing) \Delta \lambda_{trans\ dip} \frac{\partial n_{eff}(sensing)}{\partial \lambda} \right. \\ & \quad \left. \left. + \Delta n_l \frac{\partial n_{eff}(sensing)}{\partial n_l} \right) L_{sensing} \right], \end{aligned} \quad (4)$$

$$\begin{aligned} \Delta \lambda_{trans\ dip} &= \frac{2}{m} \left[ \left( \Delta \lambda_{trans\ dip} \frac{\partial n_{eff}(ref)}{\partial \lambda} \right) L_{ref} \right. \\ & \quad - \left( \Delta \lambda_{trans\ dip} \frac{\partial n_{eff}(sensing)}{\partial \lambda} \right. \\ & \quad \left. \left. + \Delta n_l \frac{\partial n_{eff}(sensing)}{\partial n_l} \right) L_{sensing} \right], \end{aligned} \quad (5)$$

Using equations (2) and (4), we deduce the following equation (6)

$$\begin{aligned} & \frac{\Delta n_l}{\Delta \lambda_{trans\ dip}} \frac{\partial n_{eff}(sensing)}{\partial n_l} \lambda_{trans\ dip} L_{sensing} \\ &= \left[ \left( n_{eff}(ref) \lambda_{trans\ dip} \frac{\partial n_{eff}(ref)}{\partial \lambda} \right) L_{ref} \right. \\ & \quad \left. - \left( n_{eff}(sensing) - \lambda_{trans\ dip} \frac{\partial n_{eff}(sensing)}{\partial \lambda} \right) L_{sensing} \right], \end{aligned} \quad (6)$$

Employing ( $i = ref, sensing$ ), we can write

$$n_g(i) \text{ group index} = n_{eff}(i) - \lambda \frac{\partial n_{eff}(i)}{\partial \lambda}, \quad (7)$$

Based on the quasi TE mode in waveguide sensing arm and reference arm, the equation (5) and equation (6) are reduced as equation 8.

Optical path differences in polymer waveguide is  $[n_{g ref} L_{ref} - n_{g sensing} L_{sensing}]$ . The MZI sensitivity of the proposed polymer gradient rib-slot waveguide is defined.

$\Delta \lambda_{trans dip} / \Delta n_i$ , thus the equation (7) is derived as:

$$Sensitivity_{MZI} = \frac{\Delta \lambda_{trans dip}}{\Delta n_i} = \frac{\lambda_{trans dip}}{[n_{g ref} L_{ref} - n_{g sensing} L_{sensing}]} \frac{\partial n_{eff}(sensing)}{\partial n_i} L_{sensing}, \quad (8)$$

From equation (8) we derive MZI sensitivity which is related to sensing arm and reference arm. MZI sensitivity represents performances of sensor, comparable sensitivity with conventional silicon and silicon nitride waveguide [33].

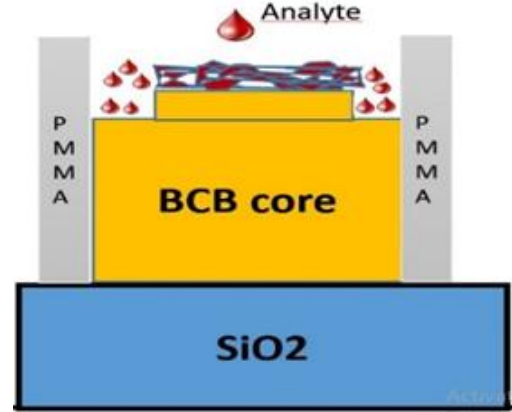


Fig. 2. (a) BCB core cross-section (color online)

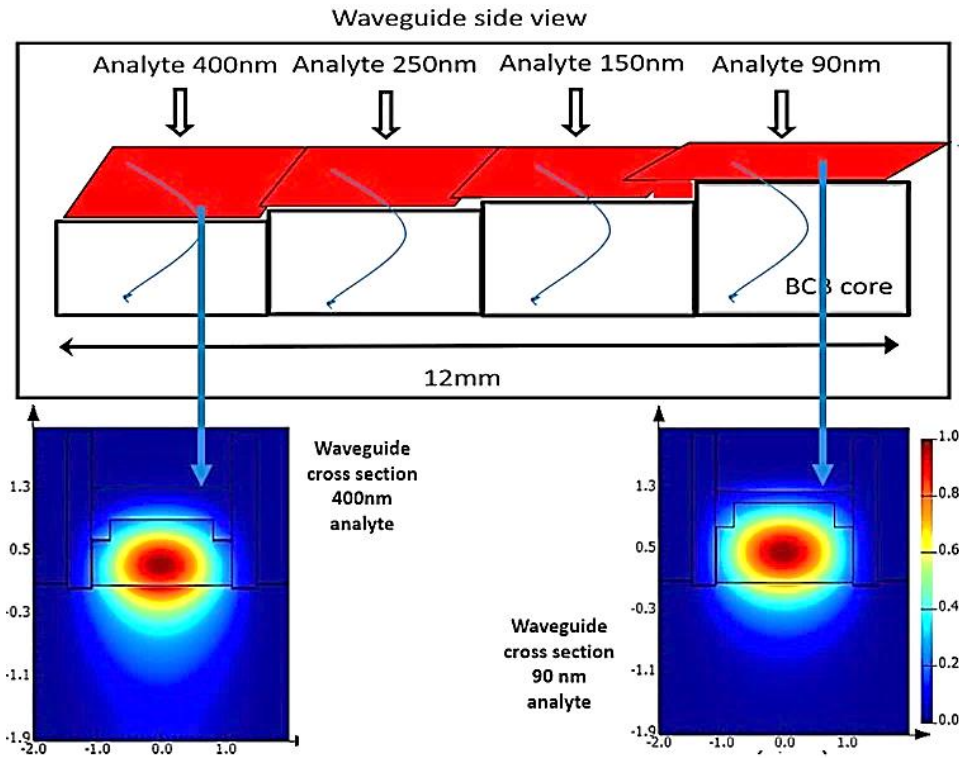


Fig. 2. (b) Waveguide side view with 400 nm analyte thickness and 90 nm thickness (color online)

### 3. Results and discussions

The proposed polymer BCB of 1  $\mu\text{m}$  thick is spin coated on silicon wafer. After curing time, BCB layer can be patterned for required sensor architecture. The proposed MZI is realized by photolithographic process, this process is carried out on polymer BCB by using transformer coupled plasma etching with mixture of different gases in to chamber. We add the PMMA cladding layer over the

BCB material. Thereafter PMMA cladding is etched in sensing arm which effectively holds the sample and avoid leakage at edges of waveguide. This PMMA will create the sensing window to improve the analyte interaction. Due to fabrications tolerance the proposed geometry will change in dimensions slightly more, this will impact the sensitivity and dip in transmission spectrum. Based on this aspect we increased the width by 200 nm and thickness by 20 nm in this proposed sensor, due to which sensitivity

increases by ten percent more. To validate the MZI sensor sensitivity, the key elements are length of sensing arm

$L_{\text{sensing}}$  1.2 cm and reference arm  $L_{\text{ref}}$  1 cm are designed for best optical path difference (OPD).

Table 1. Calculated effective index and group index for proposed MZI

Blood sample	Refractive index	$n_{\text{eff}}(\text{ref})$ effective index	$n_{\text{eff}}(\text{sensing})$ effective index	$n_g(\text{ref})$ group index	$n_g(\text{sensing})$ group index
Normal [34]	1.35	1.44689	1.457671	1.5483	1.5485
McF-7 Breast cancer [34]	1.401	1.44991	1.458597	1.5412	1.5495
Influenza A [36]	1.48	1.44689	1.467367	1.5517	1.5553

Cross section of proposed polymer waveguide with PMMA and BCB core shown in Fig. 2 (a) and the sensitivity of the MZI was calculated over dip in transmission spectrum with different disease analyte and the same are plotted.

### 3.1. Analyte transportation in waveguide

Using biological sample in the sensing arm where the analyte interacts with electromagnetic field. The biosensor uses minimal volume of liquid sample, in general C-protein (CPR) in human serum weighs 115 kilodalton per molecule. Due to the density and viscosity of the biomolecule, the spread of this sample over the waveguide surface will be not be uniform due to this a sensor cannot measure the accurate sensitivity [33]. In this polymer waveguide surface analyte thickness changes, due to this reaction of quasi-TE mode also vary. This can be described in equation (9) by temporal variation and spatial variations of sample in sensing arm.

$$\frac{\partial[\text{Analyte}]}{\partial t} + u \frac{\partial[\text{Analyte}]}{\partial x} + v \frac{\partial[\text{Analyte}]}{\partial y} = D \left( \frac{\partial^2[A]}{\partial x^2} + \frac{\partial^2[A]}{\partial t^2} \right) + G, \quad (9)$$

The analyte concentration we proposed is from the Refractive index Table 1 [34]. Bulk Analyte concentration, Diffusion (D) coefficient of analyte sample, G reaction of sample molecule in waveguide surface [35], [37]. We analyzed Electromagnetics field variation for different analyte from 400 nm to 90 nm thickness to enhance the sensitivity in physical environment. For rib -slot polymer waveguide structure, we computed effective index for sensing arm and reference arm with group effective index in FDTD and tabled in Table 1. We analyzed this sensor setup in Lumerical INTERCONNECT with all electro-optical system for plotting transmission spectra and foundry specific which validates the fabrication possibility of the biosensor.

### 3.2. Proposed Gradient rib -slot waveguide

In proposed MZI polymer waveguide sensor with asymmetric design configuration reference arm and sensing arm with different lengths. The dimensions for

better guiding structure provides enhanced confinement factor. This PMMA structure holds analyte effectively without leakage of samples at waveguide edges. The effective index of the reference arm with BCB core and PMMA cladding height of  $h = 1 \mu\text{m}$  and width  $W_{\text{ref}} = 2.5 \mu\text{m}$ , are computed and listed in Table 1. Transmission spectrum of normal cell (RI = 1.35) and cancer cell (RI= 1.401) are plotted in Fig. 4, absorption at 1555 to 1576 nm clearly show this sensor detects the cancer cell over normal cell. In Fig. 6, transmission spectrum of normal cell (RI =1.35) and Influenza A virus (RI=1.48) are plotted with absorption at 1576 nm. Optimization of waveguide structure for increased sensitivity is based on reaction of mode field in both sensing arm and reference arm of polymer surface. In Fig. 3 we analyzed mode field for rib-slot waveguide for sensing arm with different analyte thickness ranging from 400 nm to 90 nm shown in Fig. 3 (a),(b),(c),(d). Based on above equation (8) sensitivity of polymer MZI waveguide structure is calculated and it is found to be  $2.5 \times 10^5 \text{ nm/RIU}$ . The loss for this proposed polymer waveguide in Fig. 5 and Fig. 7, is dB/cm. For biosensing applications the loss can be compensated by the biosample interaction. In Table 2 the sensitivity of MZI are compared with other refractive index sensor [38], [39], [27], [35], the proposed polymer gradient rib-slot waveguide with BCB core and PMMA substrate as sample holder gives high sensitivity. These numerical analyses clearly demonstrate that, the optimizing the length of both the arms decreases the OPD between the two MZI arms.

In photonic refractive index sensor, the performance depends on TE polarization on waveguide surface based on change in analyte refractive index. In traditional silicon and silicon nitride waveguides, the confinement of light in the waveguide structure are executed with different grating couplers [40][41][42]. The suitable grating coupler proposed in [43] and [44] the same parameter is used in our proposed polymer waveguide which makes biosensors more efficient in detecting cancer and Influenza A-type virus [51]. Integrating this MZI sensor architecture in Point of care biosensor devices be more effective in detection of diseases more effective than conventional materials like silicon, silicon nitride, and cost effective. Based on cost effective parameters the fabrication process is easy and suitable for mass production when COVID – 19 pandemic-like situations in future.

Table 2. Different sensitivity analysis of MZI

Year	MZI sensor	Sensitivity	References
2009	Wavelength dip Shift method	$5 \times 10^4$	[45]
2013	Silicon nitride based slot waveguide	2663 $\pi$ /cm RIU	[46]
2014	Vernier effect	21500 nm/RIU	[47]
2015	Double –slot photonic hybrid waveguide structure	1061 nm/RIU	[48]
2017	Hollow hybrid in sensing arm waveguide	160 nm /RIU	[49]
2017	Optical waveguide over metal under cladding	5280 nm/RIU	[50]
2019	Subwavelength grating waveguide structure	598.6 nm/RIU	[38]
2019	Plasmonics co-integrated over silicon nitride	1973 nm/RIU	[39]
2020	Polymer based Horizontal slot waveguide	17024 nm /RIU	[27]
2023	Polymer SU8 and BCB Horizontal slot waveguide with optimized reference arm	19280 nm/RIU	[40]
2023	This proposed work polymer BCB core with PMMA cladding	$2.5 \times 10^5$ nm/RIU	

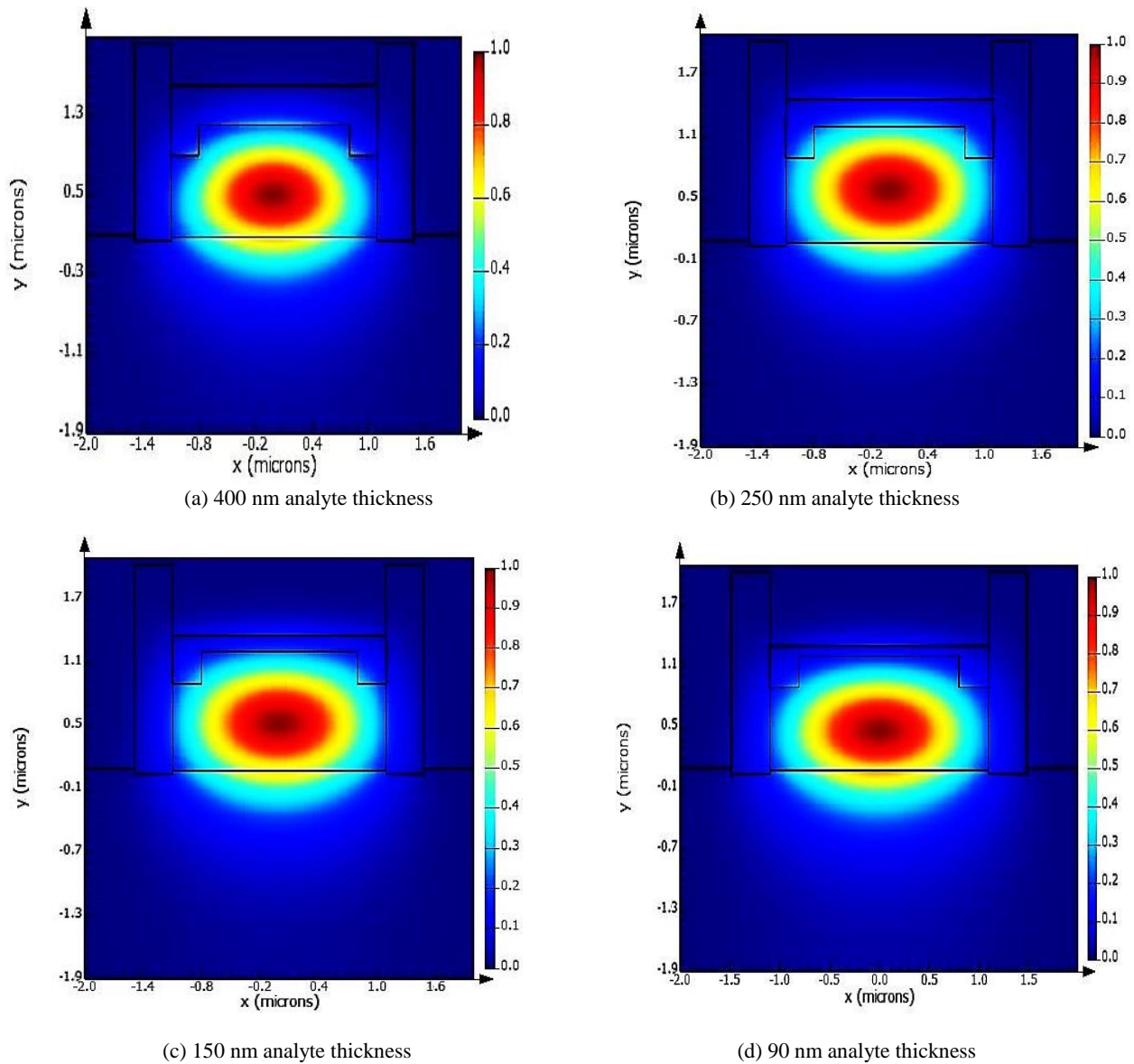


Fig. 3. Mode field analysis of rib –slot waveguide with different analyte thickness (a) 400 nm analyte thickness (b) 250 nm analyte thickness, (c) 150 nm analyte thickness, (d) 90 nm analyte thickness (color online)

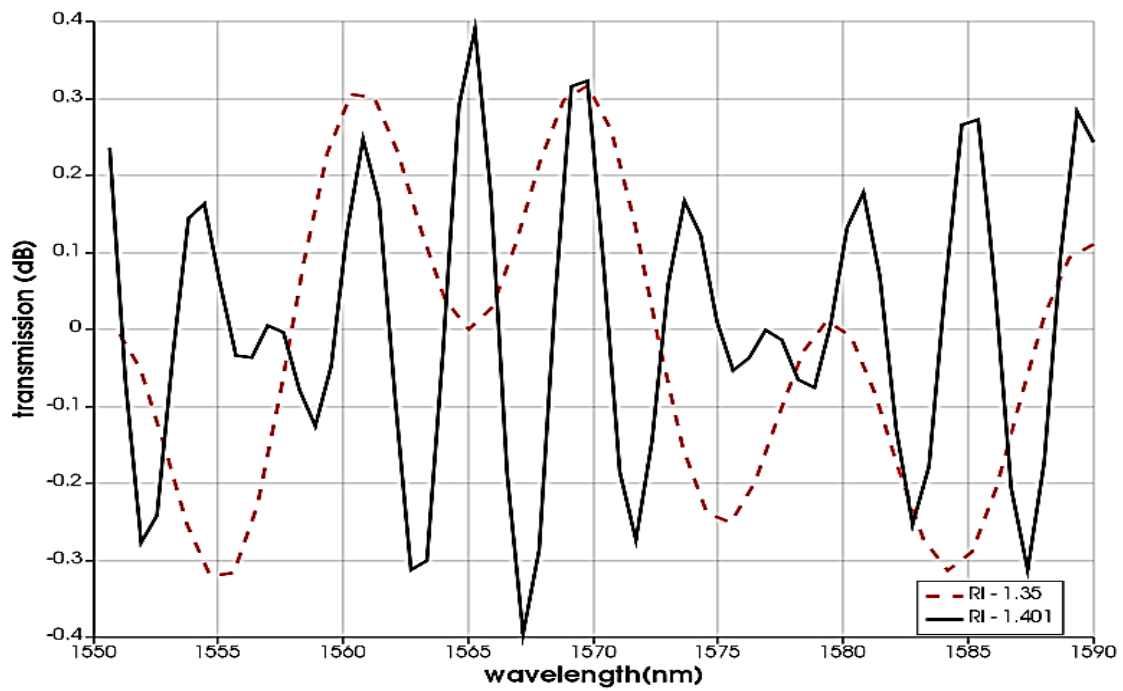


Fig. 4. Transmission Spectra of normal human cell Vs breast cancer cell (MCF-7) with refractive index of 1.401 (color online)

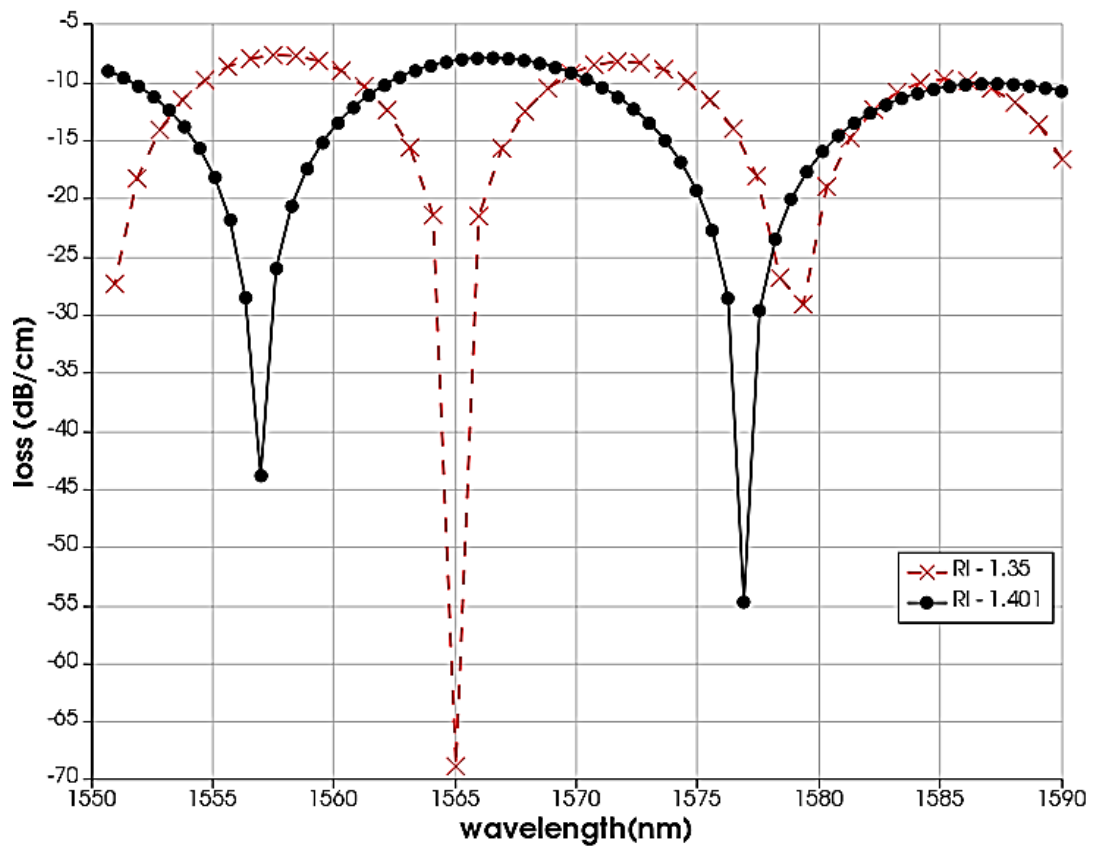


Fig. 5. Spectral response of normal human cell Vs breast cancer cell (MCF-7) with refractive index of 1.401 (color online)

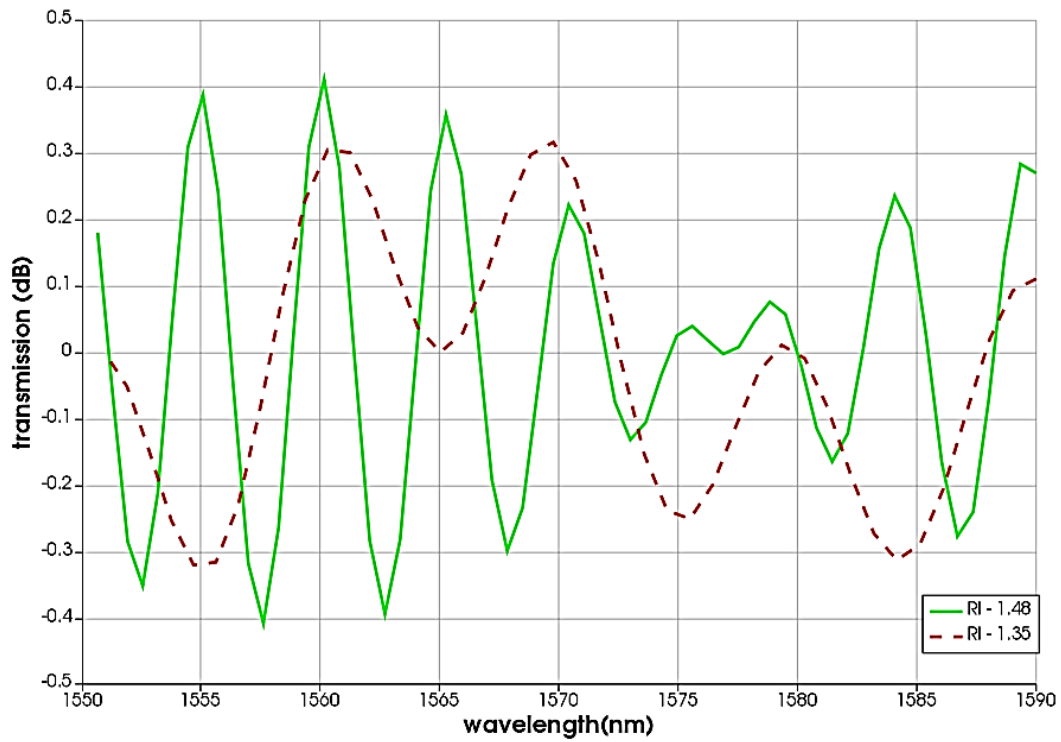


Fig. 6. Transmission Spectra of normal human cell VS influenza with refractive index of 1.48 (color online)

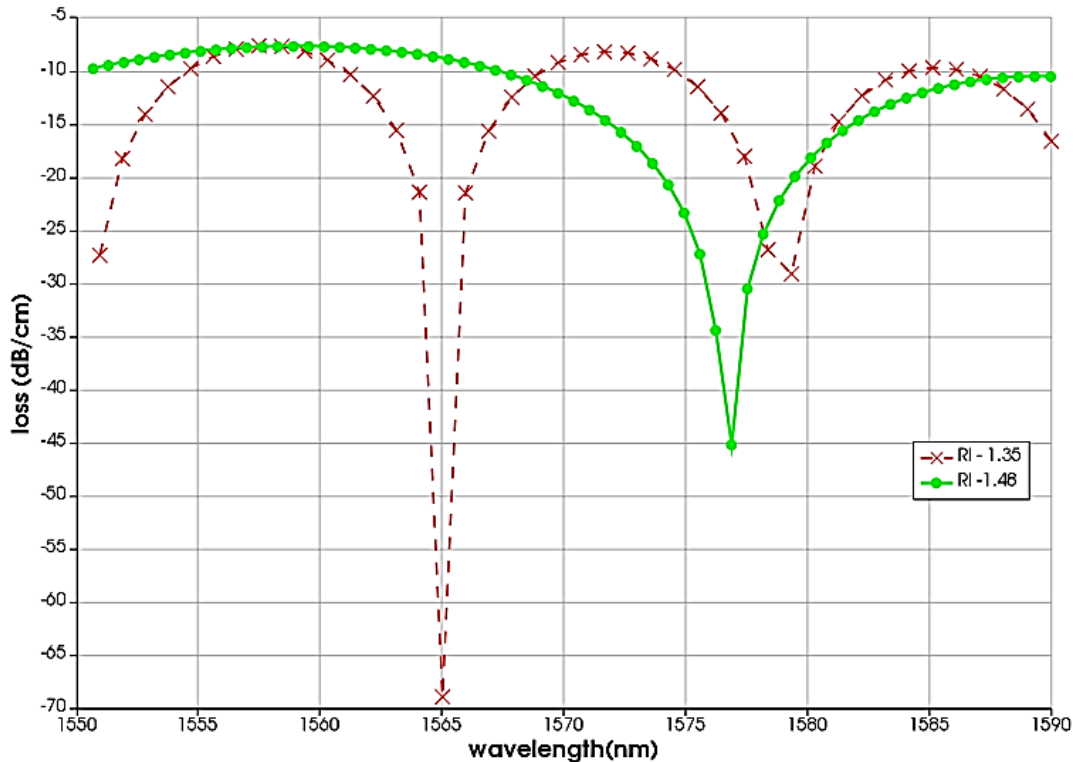


Fig. 7. Spectra response of normal human cell VS influenza with refractive index of 1.48 (color online)

#### 4. Conclusions

The proposed polymer gradient rib-slot MZI refractive index biosensor, as device could be integrated in

point of care device for detection of diseases without any laboratory setup. Our simulated results on optimized waveguide geometry maximize the MZI sensitivity based on real-time analyte reaction over waveguide surface. In

MZI sensing arm refractive index of cancer cell (1.401) and Influenza A (1.48) are applied at wavelength of 1550 nm. Proposed polymer BCB core waveguide with PMMA as sample holder is a novel waveguide structure which enhances the sensor sensitivity ( $2.5 \times 10^5$ ) nm/RIU, compared to other MZI conventional waveguide structure. The advantages of this proposed polymer refractive index sensor are cost effective in terms of fabrication and material. This proposed biosensor can detect Influenza A type and cancer cells in short time and possibility of mass fabrication in pandemic-like emergency situations.

### Author Contributions

Design and simulation analysis were performed by Prasanna Kumar. The manuscript preparation was performed by Prasanna Kumar and Sivasubramanian.

### Data Availability Statement

The data underlying the results presented in this paper are not publicly available at this time but may be obtained from the authors upon reasonable request.

### Conflicts of Interest

The authors declare no conflicts of interest.

### Acknowledgments

This proposed work was performed in the Fiber Optics Laboratory on Lumerical software provided by Vellore Institute of Technology, Chennai.

### References

- [1] H. Sakamoto, Y. Minpou, T. Sawai, Y. Enami, S. Suye, *Appl. Biochem. Biotechnol.* **178**(4), 687 (2016).
- [2] ICMR- National Centre for Disease Informatics and Research, "Report of the National Cancer Registry Programme (2012-2016)," pp. 1–282, 2020.
- [3] B. Hossain, A. K. Paul, Md. A. Islam, Md. M. Rahman, A. K. Sarkar, L. F. Abdulrazak, *Optik* **252**, 168506 (2022).
- [4] M. M. Ariannejad, J. D. Tan, C. C. Kang, M. Ghasemi, P. K. Choudhury, *The European Physical Journal D* **76**(5), 91 (2022).
- [5] Y. Xie, M. Zhang, D. Dai, *Sensors* **20**(9), 2640 (2020).
- [6] Y. Liu, Q. Liu, S. Chen, F. Cheng, H. Wang, W. Peng, *Sci. Rep.* **5**(1), 12864 (2015).
- [7] Brit M. Quandt, Fabian Braun, Damien Ferrario, René M. Rossi, Anke Scheel-Sailer, Martin Wolf, Gian-Luca Bona, Rudolf Hufenus, Lukas J. Scherer, Luciano F. Boesel, *J. R. Soc. Interface* **14**(128), 20170060 (2017).
- [8] Varnakavi Naresh, N. Lee, *Sensors* **21**(4), 1109 (2021).
- [9] C. Chen, J. Wang, *Analyst.* **145**(5), 1605 (2020).
- [10] S. Parra, E. Carranza, J. Coole, B. Hunt, C. Smith, P. Keahey, M. Maza, K. Schmeler, *IEEE J. Transl. Eng. Health Med.* **8**, 1 (2020).
- [11] X. Fan, I. M. White, S. I. Shopova, H. Zhu, J. D. Suter, Y. Sun, *Anal. Chim. Acta* **620**(1–2), 8 (2008).
- [12] D. Duval, J. Osmond, S. Dante, C. Dominguez, L. M. Lechuga, *IEEE Photonics J.* **5**(2), 3700108 (2013).
- [13] E. Luan, H. Shoman, D. Ratner, K. Cheung, L. Chrostowski, *Sensors* **18**(10), 3519 (2018).
- [14] C. Zhao, L. Xu, L. Liu, *Sensors* **21**(19), 6600 (2021).
- [15] N. L. Kazanskiy, S. N. Khonina, M. A. Butt, *Photonics* **9**(5), 331 (2022).
- [16] R. S. El Shamy, M. A. Swillam, X. Li, *Sci. Rep.* **12**(1), 9343 (2022).
- [17] A. Crespi, Y. Gu, B. Ngamsom, H. J. W. M. Hoekstra, C. Dongre, M. Pollnau, R. Ramponi, *Lab on a Chip* **10**(9), 1167 (2010).
- [18] O. Lazcka, F. J. Del Campo, F. X. Muñoz, *Biosens. Bioelectron.* **22**(7), 1205 (2007).
- [19] X. Zhang, G. Zhou, P. Shi, H. Du, T. Lin, J. Teng, F. S. Chau, *Opt. Lett.* **41**(6), 1197 (2016).
- [20] A. R. Bastos, C. M. S. Vicente, R. Oliveira-Silva, N. J. O. Silva, M. Tacão, J. P. Costa, M. Lima, P. S. André, *Sensors* **18**(3), 840 (2018).
- [21] Y. Ma, N. Nguyen-Huu, J. Zhou, H. Maeda, Q. Wu, M. Eldlio, J. Pištora, M. Cada, *IEEE Journal of Selected Topics in Quantum Electronics* **23**(4), 1 (2017).
- [22] F. Qiu, Andrew. M. Spring, J. Hong, S. Yokoyama, *Opt. Express* **26**(9), 11213 (2018).
- [23] G. Roelkens, D. Van Thourhout, R. E. Baets, *Electron. Lett.* **41**(9), 561 (2005).
- [24] Y. Liu, Y. Sun, Y. J. Yi, L. Tian, Y. Cao, C. M. Chen, X. Q. Sun, D. M. Zhang, *Chinese Physics B* **26**(12), 124215 (2017).
- [25] M. Hofmann, Y. Xiao, S. Sherman, U. Gleissner, T. Schmidt, H. Zappe, *Appl. Opt.* **55**(5), 1124 (2016).
- [26] C. Li, J. Liu, Z. Chi, H. Zhang, X. Peng, *Proceedings of IEEE Sensors* **2018**, 1–4 (2018).
- [27] X. Ma, K. Chen, J. Wu, L. Wang, *Photonic Sensors* **10**(1), 7 (2020).
- [28] S. Wang, X. Shan, U. Patel, X. Huang, J. Lu, J. Li, N. Tao, *Proceedings of the National Academy of Sciences* **107**(37), 16028 (2010).
- [29] Q. Liu, X. Tu, K. W. Kim, J. S. Kee, Y. Shin, K. Han, Y. J. Yoon, G. Q. Lo, M. K. Park, *Sens. Actuators B Chem.* **188**, 681 (2013).
- [30] M. Selmi, M. H. Gazzah, H. Belmabrouk, *Sci. Rep.* **7**(1), 5721 (2017).
- [31] J. Milvich, D. Kohler, W. Freude, C. Koos, *Opt. Express* **26**(16), 19885 (2018).
- [32] S. Prasanna Kumar, A. Sivasubramanian, *Journal of Healthcare Engineering* **2021**, article ID 6081570 (2021).

- [33] S. Prasanna Kumar, A. Sivasubramanian, *Int. J. Opt.* **2022**, 1 (2022).
- [34] X. J. Liang, A. Q. Liu, X. M. Zhang, P. H. Yap, T. C. Ayi, H. S. Yoon, The 13th International Conference on Solid-State Sensors, Actuators and Microsystems, Digest of Technical Papers. TRANSDUCERS '05 Seoul, Korea (South), IEEE, 1712 (2005).
- [35] R. S. El Shamy, M. A. Swillam, X. Li, *Sci. Rep.* **12**(1), 9343 (2022).
- [36] S. Wang, X. Huang, X. Shan, K. J. Foley, N. Tao, *Analytical Chemistry* **82**(3), 935 (2010).
- [37] M. Selmi, M. H. Gazzah, H. Belmabrouk, *Sci. Rep.* **7**(1), 5721 (2017).
- [38] M. Odeh, K. Twayana, K. Sloyan, J. E. Villegas, S. Chandran, M. S. Dahlem, *IEEE Photonics J.* **11**(5), 1 (2019).
- [39] A. Manolis, E. Chatzianagnostou, G. Dabos, N. Pleros, B. Chmielak, A. L. Giesecke, C. Porschatis, *Opt. Express* **27**(12), 17102 (2019).
- [40] S. Prasanna Kumar, A. Sivasubramanian, *Sensors International* **4**, 100207 (2023).
- [41] A. Kumar, S. Nambiar, R. Kallega, P. Ranganath, P. Ea, S. K. Selvaraja, *Opt. Express* **29**(7), 9699 (2021).
- [42] S. Prasanna Kumar, A. Sivasubramanian, *Sensors International* **5**, 100255 (2024).
- [43] S. Prasanna Kumar, A. Sivasubramanian, *Springer Proceedings in Physics*, Springer, Singapore **258**, 695 (2021).
- [44] S. Prasanna Kumar, A. Sivasubramanian, *Int. J. Opt.* **2022**, 1 (2022).
- [45] R. Levy, S. Ruschin, D. Goldring, *Opt. Lett.* **34**(19), 3023 (2009).
- [46] Q. Liu, K. S. Chiang, V. Rastogi, *Journal of Lightwave Technology* **21**(12), 3399 (2003).
- [47] X. Jiang, Y. Chen, F. Yu, L. Tang, M. Li, J.-J. He, *Opt. Lett.* **39**(22), 6363 (2014).
- [48] X. Sun, D. Dai, L. Thylén, L. Wosinski, *Opt. Express* **23**(20), 25688 (2015).
- [49] X. Sun, L. Thylén, L. Wosinski, *Opt. Lett.* **42**(4), 807 (2017).
- [50] R. Dwivedi, A. Kumar, *Sens. Actuators B Chem.* **240**, 1302 (2017).
- [51] S. Prasanna Kumar, A. Sivasubramanian, *Sensors International* **4**, 100207 (2023).

---

\*Corresponding authors: pkprajan7196@gmail.com  
sivasubramanian.a@vit.ac.in